Proceedings of the 29th Annual International
Conference of the IEEE EMBS
Cité Internationale, Lyon, France
August 23-26, 2007.

Towards the Control of Individual Fingers of a Prosthetic Hand Using Surface EMG Signals

Francesco Tenore*, Ander Ramos*,
Amir Fahmy, Soumyadipta Acharya, Ralph Etienne-Cummings,and Nitish V. Thakor

Abstract— **The fast pace of development of upper-limb prostheses requires a paradigm shift in EMG-based controls. Traditional control schemes are only capable of providing 2 degrees of freedom, which is insufficient for dexterous control of individual fingers. We present a framework where myoelectric signals from natural hand and finger movements can be decoded with a high accuracy. 32 surface-EMG electrodes were placed on the forearm of an able-bodied subject while performing individual finger movements. Using time-domain feature extraction methods as inputs to a neural network classifier, we show that 12 individuated flexion and extension movements of the fingers can be decoded with an accuracy higher than 98%. To our knowledge, this is the first instance in which such movements have been successfully decoded using surface-EMG. These preliminary findings provide a framework that will allow the results to be extended to non-invasive control of the next generation of upper-limb prostheses for amputees.**

I. INTRODUCTION

According to the National Institutes of Health (NIH), there are approximately 1.9 million people living with limb loss in the United States. It is estimated that there are 50,000 new amputations every year and a quarter of them are from the upper limb. Partial hand amputation, with loss of 1 or more fingers, is the most prevalent upper limb amputation. Since hand and finger dexterity requires muscles in the forearm and since $\sim$70% of all upper limb amputations are distal to the elbow [1], [2], this makes the case for the development of hand prostheses with a high degree of dexterity.

However, most of the current commercially available prostheses that help overcome the loss of a limb use surface myoelectric signals (MES) signals to control a very limited number of degrees of freedom (DOF) (< 3) [3], [4]. New breakthroughs and developments in the next generation of high dexterity prosthetic arms have made this control insufficient. Prosthetic hands like the Utah/MIT dexterous hand, Shadow dexterous hand, Cyberhand, DLR-HIT hand or the Fluid hand with more than 16 DOF's offer a higher degree of control (see [5] for a summary of many prosthetic hands under development). While these prosthetic devices are not far from market, no noninvasive-EMG control system offers the high level of control required by the devices [6].

Some groups have demonstrated that a higher dexterity EMG-based control could be achieved using different combinations of extracted features and classification methods [7], [8], [9], [10], [11]. Better results have been shown using invasive EMG electrodes [12]. Although this procedure seems to be the future for controlling the next generation of prosthetic arms, the current-state-of the-art is still in its clinical testing phase, is invasive, subject to ethical considerations, and the long term effect of the implants is still being researched [14], [15]. Jiang et al. [13] have shown end-point control of three fingers using features from the wavelet transform of the EMG signals.

This paper aims at closing this control gap to ultimately enable individual finger movements on the next generation of prostheses. We present surface EMG data collected from 32 bipolar electrodes placed mainly on an able-bodied individual's forearm performing 10 individual finger movements and 2 movements of grouped fingers. Using traditional signal analysis tools we show that it is possible to achieve very high accuracy ($> 98\%$).

II. METHODS

A. Data Acquisition

EMG data was acquired using a Compumedics (El Paso, TX, USA) Neuroscan SynAmps^2 64-channel amplifier. The amplifier was connected to a PC for data storage. Auditory and visual, animated cues were presented on a computer screen and used for synchronization with the data. Sampling was performed at 2000 Hz and bandpass filtered between DC and 500 Hz.

Before electrode placement, the arm was cleaned with a Nuprep abrasive skin preparation gel from D.O. Weaver & Co., Aurora, CO, USA. The subject's arm was also shaved to avoid high impedances in the signals.

Afterwards an EMG array of 32 bipolar Ag/AgCl electrodes from Myotronics-Noromed (Tukwila, WA, USA) was placed on the arm following SENIAM recommendations [16], two Cleartrace LT reference electrodes from ConMed Corporation (Utica, NY, USA) were used as reference and ground. A reference electrode was placed on the distal part of the *olecranon* and the ground electrode was placed on the clavicle.

*These authors contributed equally to this work.

This work was supported by the Revolutionizing Prosthetics 2009 program and funded by the Defense Advanced Research Project Agency (DARPA).

Francesco Tenore, Amir Fahmy and Ralph Etienne-Cummings are with the Department of Electrical & Computer Engineering, Soumyadipta Acharya and Nitish Thakor are with the Biomedical Engineering at The Johns Hopkins University, Baltimore, USA, Ander Ramos is with the Fatronik Foundation, Research Technology Center, San Sebastian, Spain, and the Department of Biomedical Engineering, University of Munich, Munich, Germany. Corresponding author: aramos@fatronik.com

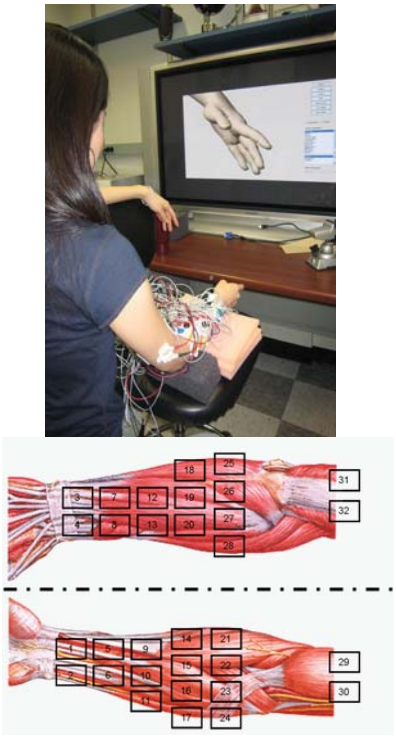

Fig. 1. Experimental setup. Top: A subject performing a trial (index extension). Bottom: Approximate location of electrodes, superimposed on Netter's pictorials [17]

B. Experimental Setup

An array of 32 bipolar EMG electrodes was placed on the subject's arm following physical landmarks, as depicted in Fig. 1b. Experiments were performed following Johns Hopkins Institutional Review Board (IRB) approval. The subject was seated in front of a 50" screen, his primary arm resting his elbow and wrist on two separate compliant surfaces to avoid artifacts generated by contact between electrodes and the resting surfaces. The arm was bent to form a 90° angle. Twelve different movements were executed by the subject in response to a visual animation on the screen and auditory cue that depicted the movement to be reproduced. The movements consisted of flexions and extensions of all the fingers individually and of the middle, ring and little finger as a group (MRP group). The movements were denominated e1, e2,..., e5, e345, f1, f2,..., f345, where e1 is extension of the thumb, and f345 is flexion of the 3 fingers as a group. Each movement was presented in a random sequence and repeated 30 times in 3 blocks of 10, with a resting period of 2 to 5 minutes between each block, to avoid fatigue. Each individual trial lasted between 5 s and 7 s. Upon presentation of the cue, the subject was asked to flex or extend a specific finger or group of fingers and then keep the position for 3 s when a rest cue was provided, lasting between 2 s and 4 s between each trial, again, to minimize fatigue. The structure of an individual trial is shown in Fig. 2.

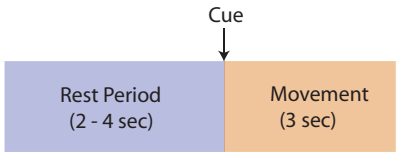

Fig. 2. Timing diagram for experimental trials

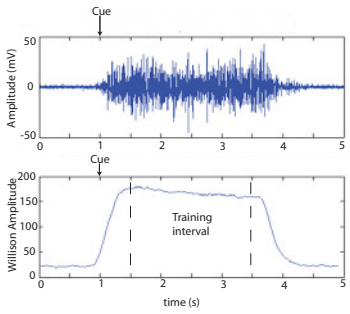

Fig. 3. Filtered EMG data for a single trial from a single electrode (top); Willison Amplitude of EMG signal (bottom). The cue is presented at the 1 s mark. Data used for training is the 2 s time interval that begins 0.5 s after the cue.

C. Signal Processing

The EMG data was bandpass filtered with a low cutoff frequency of 10Hz and a high cutoff frequency of 500 Hz as recommended by the Surface EMG for Non-Invasive Assessment of Muscles [16] protocol. The signals were acquired using a 64 unipolar channel amplifier and subsequently bipolarized subtracting the channels that correspond to the same electrode. The thirty trials were reorganized by concatenating all the same movements. The Principal Component (PC) for each movement type was extracted and used to detect eventual erroneous movements, i.e. if the subject performed a movement different from the one indicated by the visual cue. We found that this technique highlights differences between the different trials for the same movement and allows immediate identification of erroneous trials. While operator errors are a practical reality of these experiments, it brings no advantage to use them in training the neural network classifier. Therefore, after localizing these potential errors, visual inspection of the raw data was performed to ultimately reject the trials containing such errors from the training set.

D. Feature Extraction

From the raw EMG data, four frequently used time-domain EMG features were extracted [6].

Different attributes and information can be gathered from a variety of time domain features. The four that were chosen in this study were the 1) Mean of the absolute value; 2) Willison Amplitude; 3) Variance; 4) Waveform length.

1) Mean of the absolute value ($\overline{X}$): this feature displays a large increase in value at onset and maintains fairly high values during contraction.

2) Willison Amplitude (W): if x_i are the individual EMG data, then

$$W = \sum_{i=1}^{N} f(|x_i - x_{i-1}|) \quad (1)$$

where

$$f(x) = \begin{cases} 1 & \text{if x} > \text{threshold} \\ 0 & \text{otherwise} \end{cases} \quad (2)$$

The Willison Amplitude for a given interval represents the number of times that the magnitude of the difference for every two consecutive points exceeds a certain threshold. Its value correlates to muscle contraction levels [6]. An example of this feature is shown in Fig. 3 (bottom).

3) Variance (S^2): this parameter is a representation of the EMG signal power, helping to identify onset and contraction.

4) Waveform Length (WL)

$$WL = \sum_{i=1}^{N} |x_i - x_{i-1}| \quad (3)$$

The waveform length of the signal provides indicators for signal amplitude and frequency.

Additionally, the data was weighted by three trapezoidal windows, to achieve a more stable energy distribution for feature extraction, as described by Du et al. [18]. Briefly, a feature is extracted for each of the three windows. The resulting three features are then summed to obtain one final value of the feature of the 200 ms window. The length of the window was chosen to simultaneously minimize the delay between performed and decoded action while providing sufficient data for a valid feature to be extracted. Each window was shifted by 25 ms, thereby overlapping adjacent windows. This allows reasonable continuity in the extracted feature.

With reference to Fig. 3, the features actually extracted belonged to the two second interval that begins 0.5 s following the cue, which implies that each trial is characterized by 80 features, i.e. 2000 ms / 25 ms. This was done to account for delays in reaction time and to ensure that the muscles activated to perform the movement were contracted.

E. Classification

The extracted features were transformed in a Principal Component space (performing a discrete Karhunen-Love transform) to linearly separate them. Non-linear decoding filters were designed using multilayer, feed-forward Artificial Neural Networks (ANNs) because of their use in non-linear regression and classification [19]. By using a tan-sigmoid transfer function for the hidden layer neurons and a log-sigmoid for the output layer, the network assigns a probability to each movement, P$\{M_i\}$, where i = $1, ..., 12$, corresponding to the 10 individuated movements types and the MRP group movements and output the movement type with the highest probability. The neural network was trained using Matlab's scaled conjugate gradient descent algorithm in combination with early validation to improve generalization.

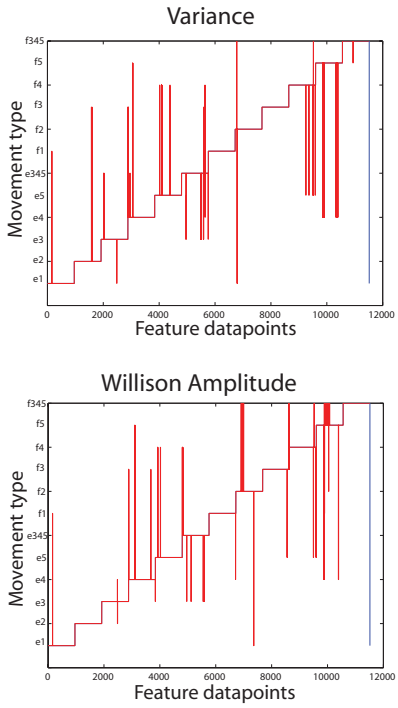

Fig. 4. Plot of actual decoded outputs for the 12 movement types using two of the features described in the text. The Feature Datapoints shown in the abscissa are the features for each 25 ms increment of the data window. The "steps" shown in the plots are the correct movements for that time interval. When a vertical red bar appears on a step, this represents a misclassification.

III. Results and Discussion

The decoding accuracy of the individual and the group movements was evaluated using each of the features described in the previous section individually. The decoding of all the features was characterized by high accuracies, on average $\geq$98% for all the features. Fig. 4 shows two classification outputs using variance (top) and Willison Amplitude (bottom) as extracted features. Fig. 5 presents the confusion matrices obtained for the same two features, and both with 60 neurons in the hidden layer. From close examination of the figure, it shows that while the overall accuracy of the movement decoding is almost perfect, two movements were not as good as the rest, and the two movements coincide for both features: the extension of the combined finger movements and the flexion of the little finger.

To elaborate, these plots give us a better understanding of potential sources of confusion between movements. For example, e1 and f1 movements are confused, albeit scarcely. This could be due to the fact that the movement of a finger is made up of a group of submovements involving different muscle groups [20]. In this case, it seems that these subcontractions are similar.

Furthermore, it is interesting to note a different type of confusion. This arises between the movement of the group of three fingers and the same movement of one of the three fingers that make up the group. Specifically, the extension of the middle finger with the extension of the group (e3 vs. e345) and the flexion of little finger with the flexion of the

group (f5 vs f345). This is probably a consequence of the nature of the movement itself, since the group movement is made up of the movement of the three individual fingers. One way to improve this type of confusion is possibly to apply a different decoding scheme in the neural network. This would consist in reducing the number of neurons in the output layer by removing the two output neurons associated with the group movements and replace them with a new probability associated with the movement of the three fingers together. Future work on this will explore this possibility.

IV. Conclusion

This work is a significant but still preliminary step towards the development of dexterous control of individual and groups of fingers in a prosthetic hand. Since all the recordings were taken proximally to the wrist, this holds great potential for achieving similar results with subjects who have withstood amputations distal to the elbow. However, fatigue and muscle atrophy associated with an amputation might result in significant differences in patterns from healthy individuals. With this in mind, data has recently been collected from a transradial amputee performing the same tasks and a detailed examination of the differences between an able-bodied person and a transradial amputee during finger movements will be undertaken. Furthermore, a reduction in the number of electrodes, without compromising accuracy, would significantly simplify the requirements for controlling the next generation of prostheses. Principal and Independent Component Analysis (PCA, ICA), for example, can help identify and remove electrodes which do not contribute enough information.

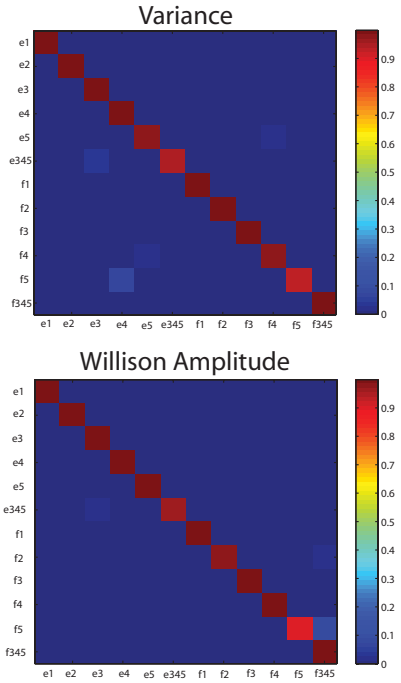

Fig. 5. Confusion matrices of data classified using the variance of the raw EMG signal (top) and the Willison Amplitude(bottom) as features, for the 12 movement types.

References

[1] T. R. Dillingham, L. E. Pezzin, E. J. MacKenzie. Limb amputation and limb deficiency: epidemiology and recent trends in the United States. *South Med J*, **95**(8); 2002.

[2] R. F. Weir, E. C. Grahn. Development of Externally-powered prostheses for persons with partial hand amputation. *Proc. IEEE EMBS International Conference*, 2000.

[3] V. S. Nelson, K. M. Flood, P. R. Bryant, M. E. Huang, P. F. Pasquina, T. L. Roberts. Limb deficiency and prosthetic management. 1. Decision making in prosthetic prescription and management. *Archives of Physical Medicine and Rehabilitation*, **87**: S3-9, 2006.

[4] R. A. Roeschlein, E. Domholdt. Factors related to successful upper extremity prosthetic use, *Prosthetics and Orthotics International*, **13**:14-8, 1989.

[5] http://www.shadowrobot.com/hand

[6] M. Zecca, S. Micera, M.C. Carrozza and P. Dario. Control of Multifunctional Prosthetic Hands by Processing the Electromyographic Signal. *Critical Review in Biomedical Engineering*, **30**(4-6):459-485, 2002.

[7] K. Englehart, B. Hudgins. A robust, real time control scheme for multifunction myoelectric control. *IEEE Trans. Biomedical Engineering*, **50**(7):848- 854, 2003.

[8] K. R. Wheeler, M. H. Chang and K. H. Knuth. Gesture-Based Control and EMG Decomposition. *IEEE Tans. on Systems, Man, and Cybernetics*, **36**(4), July 2006.

[9] K. A. Farry, I. D. Walker and R. G. Baraniuk, "Myoelectric teleoperation of a complex robotic hand," *Proc. IEEE Int. Conf. Robotics and Automation*, **12**(5):775:788, 1996.

[10] G.Wang, Z.Wang, W. Chen and Zhuang. Classification of Surface EMG signals using optimal wavelet packet method based on Davies-Bouldin criterion. *Medical and Biological Engineering and Computing* **44**:865-872, 2006.

[11] D. Peleg, E. Braiman, E. Yom-Tov, G. F. Inbar. Classification of Finger Activation for Use in a Robotic Prosthesis Arm. *IEEE Transactions on Neural Systems and Rehabilitation Engineering*, **10**(4), December 2002.

[12] T. R. Farrel and R. F. Weir. Pilot Comparison of Surface vs. Implanted EMG for Mutifunctional Prosthesis Control. *IEEE 9th Int. Conf. on Rehab. Robotics*, 2005.

[13] M. W. Jiang, R. C. Wang, J. Z. Wang, D. W. Jin. A Method of Recognizing Finger Motion Using Wavelet Transform of Surface EMG Signal. *IEEE-Engineering in Medicine and Biology Society*, 2005.

[14] S. Rodot, R. Capurro. Ethical aspects of ICT implants in the human body. *European Group on Ethics in Science and new technologies to the European Commission*. Opinion, No 20, March 2005.

[15] E. C. Leuthardt, G. Schalk, D. Moran, J. G. Ojemann. The Emerging World of Motor Neuroprosthetics: A Neurosurgical Perspective. *Neurosurgery*, **59**(1):1-14, 2006.

[16] J. H. Blok, D. F. Stegeman. Simulated bipolar SEMG characteristics. Hermens HJ, Freriks B, editors. *SENIAM 5: The state of the art on sensors and sensor placement procedures for surface electromyography: a proposal for sensor placement procedures*, ISBN 90-75452-09-8, 1997.

[17] F. H. Netter. Atlas of Human Anatomy. *Saunders*. IV edition.

[18] S. Du, M. Vuskovic. Temporal vs. spectral approach to feature extraction from prehensile EMG signals. *IEEE Information Reuse and Integration*, 2004.

[19] S. Haykin. Neural Networks: A comprehensive foundation (2^{nd} Edition. *Prentice Hall*, 1999.

[20] W. G. Darling, K. J. Cole. Muscle activation patterns and kinetics of human index finger movements. *J Neurophysiol* **63**:10981108, 1990.